Universal Parametrization of Thermal Photon Rates in Hadronic Matter

Matthew Heffernan,[1,2,*] Paul Hohler,[1,†] and Ralf Rapp[1,‡]

[1] *Cyclotron Institute and Department of Physics and Astronomy, Texas A&M University, College Station, TX 77843-3366, USA*

[2] *Department of Physics, College of William & Mary, Williamsburg, VA 23187-8795, USA*

Electromagnetic (EM) radiation off strongly interacting matter created in high-energy heavy-ion collisions (HICs) encodes information on the high-temperature phases of nuclear matter. Microscopic calculations of thermal EM emission rates are usually rather involved and not readily accessible to broad applications in models of the fireball evolution which are required to compare to experimental data. An accurate and universal parametrization of the microscopic calculations is thus key to honing the theory behind the EM spectra. Here we provide such a parametrization for photon emission rates from hadronic matter, including the contributions from in-medium ρ mesons (which incorporate effects from anti-/baryons), as well as Bremsstrahlung from $\pi\pi$ scattering. Individual parametrizations for each contribution are numerically determined through nested fitting functions for photon energies from 0.2 to 5 GeV in chemically equilibrated matter of temperatures 100-180 MeV and baryon chemical potentials 0-400 MeV. Special care is taken to extent the parameterizations to chemical off-equilibrium as encountered in HICs after chemical freezeout. This provides a functional description of thermal photon rates within a 20% variation of the microscopically calculated values.

Introduction. The understanding of hot and dense QCD matter remains a primary goal in nuclear physics. This is experimentally pursued through ultra-relativistic heavy-ion collisions (URHICs), producing a fireball of strongly interacting matter which expands and cools. Photons are an interesting probe of this fireball because they are emitted throughout its lifetime and reach the detectors without further interactions with the medium, see Refs. [1, 2] for recent reviews. The experimentally measured spectra depend on both the microscopic production mechanisms and the bulk evolution of the fireball. Recent measurements of direct-photon spectra and their elliptic flow [3–7] have triggered intense activity to understand the data [8–18]. In particular, the magnitude of the elliptic flow points to large contributions from intermediate and late phases of the fireball evolution, i.e., the pseudo-critical region and the hadronic phase [9].

In the present paper, we focus on thermal emission from the hot and dense hadronic medium. Early works on this problem have concentrated on hot meson matter [19–22]; a rather detailed analysis of the $\pi\rho a_1$ system (with an extension to strangeness) has been conducted in Ref. [23], where pertinent rate parameterizations in photon energy (q_0) and temperature (T) have also been given. Based on developments in the dilepton sector [24, 25], it was realized that baryonic emission sources play an important role for photon rates, by carrying the in-medium ρ spectral function to the photon point [23]. The underlying many-body calculations of the ρ spectral function, which account for pion-cloud modifications (corresponding to pion exchange reactions, including Bremsstrahlung) and resonant ρ-hadron interactions (corresponding to resonance Dalitz decays) [25–27], are rather involved and as such not readily available for a broad use in evolution models of URHICs. The main objective of the present paper is to provide compact parameterizations of these photon rates which for the first time encompass a finite baryon chemical potential (μ_B) as an additional variable. We also revisit the problem of hadronic Bremsstrahlung, specifically for the most abundant $\pi\pi \to \pi\pi\gamma$ channel, by extending the calculations of Ref. [28] to higher energies and providing pertinent parameterizations as well.

Thermal photon rate parametrizations. We first consider thermal photons emitted from in-medium ρ mesons; the pertinent rates can be cast in terms of the transverse electromagnetic (EM) spectral function, $\rho_{\rm EM}^T$, as [29]

$$q_0 \frac{dR_\gamma}{d^3q}\,(q_0;\mu_B,T) = \frac{\alpha_{\rm EM}}{\pi} f^B(q_0;T)\rho_{\rm EM}^T(q_0=q;\mu_B,T) \tag{1}$$

with $f^B(q_0;T) = 1/[e^{(q_0/T)}-1]$: Bose distribution function, and $\alpha_{\rm EM}$=1/137. By invoking (a generalized) vector meson dominance, the EM spectral functions can be related to the in-medium ρ propagator. The latter has been developed in Refs. [24–27] and leads to a strong broadening of the spectral peak due to interactions with baryons and anti-baryons, which are critical in describing experimental dilepton spectra from URHICs [30]. Photon rates are readily extracted from the light-like limit of vanishing invariant mass, $M \to 0$, and depend on energy, q_0, temperature, T, and baryon chemical potential, μ_B.

In a first step of constructing a parametrization, the photon emission rates have been explicitly calculated [26] at μ_B=0 for a set of 9 temperatures, T=100, 110, ..., 180 MeV, shown by the symbols in Fig. 1 (note that these rates include effects due to (equal densities of) baryons and anti-baryons, whose contribution, however, is strongly suppressed by the thermal weight as T decreases). These rates are then parameterized at each temperature by the ansatz

$$q_0 \frac{dR_\gamma^\rho}{d^3q}\,(q_0;0,T) = \exp\left[a\,(T)\,q_0 + b\,(T) + \frac{c\,(T)}{q_0+0.2}\right], \tag{2}$$

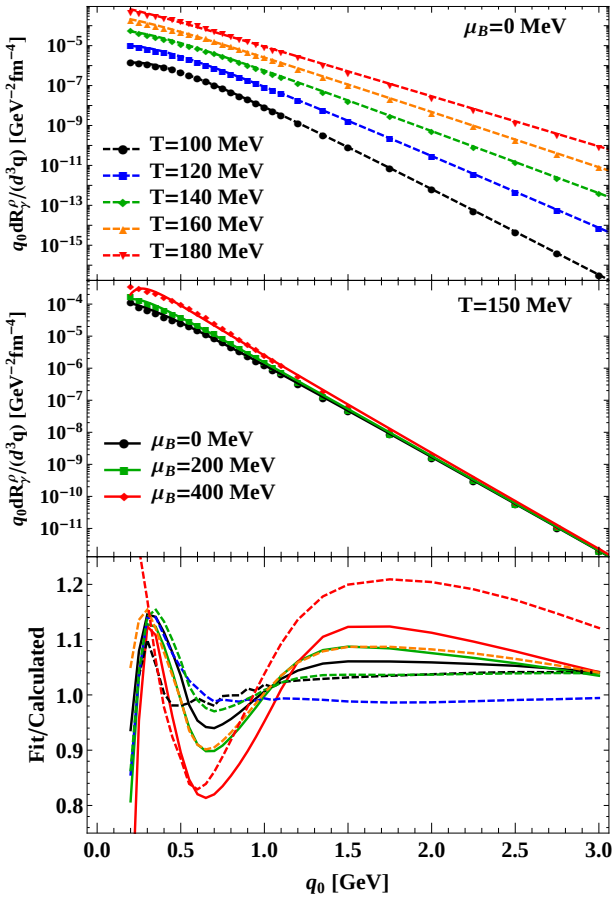

FIG. 1: Photon emission rates (vs. photon energy) calculated from in-medium ρ mesons (points) compared to their parametrization, Eq. (4) (curves), at μ_B=0 (upper panel) and T=150 MeV (middle panel). Bottom panel: Ratio of parametrization over calculated rates.

and smooth T dependencies of the parameters are found as

$$\begin{aligned} a\,(T) &= -31.21 + 353.61T - 1739.4T^2 + 3105T^3, \\ b\,(T) &= -5.513 - 42.2T + 333T^2 - 570T^3, \\ c\,(T) &= -6.153 + 57T - 134.61T^2 + 8.31T^3\ . \end{aligned} \tag{3}$$

In all parametrizations, q_0, T, and μ_B are in units of GeV. The fit results are indicated by the symbols in the upper panel of Fig. 1, and their ratio over the calculated results is displayed in the bottom panel. For the highest temperature of T=180 MeV, the deviations can reach up to 20%, but are within about 10% for all other temperatures and energies up to 5 GeV (note that the blue-shift due to the radial fireball expansion in URHICs implies an appreciable shift of the restframe energy to the lab energy, e.g., by about a factor of 2 in Au-Au($\sqrt{s}$=200 GeV) at RHIC energies [31]).

In a second step, the microscopic rates are calculated for three finite baryon chemical potentials, μ_B=0.1, 0.2 and 0.4 GeV, and for each one at the nine temperatures quoted above. Based on the μ_B=0 fits above, the following factorized ansatz was made

$$q_0 \frac{dR_\gamma^\rho}{d^3q}\,(q_0;\mu_B,T) = q_0 \frac{dR_\gamma^\rho}{d^3q}\,(q_0;0,T)\,F^\rho\,(q_0;\mu_B,T) \tag{4}$$

with the function

$$F^\rho\,(q_0;\mu_B,T) = \exp\left[d\,(\mu_B,T) - \frac{k\,(\mu_B,T)}{q_0^2} - \frac{m\,(\mu_B,T)}{q_0}\right]. \tag{5}$$

The parameters d, k, and n are determined from fits at fixed T to determine their μ_B dependence through an expansion as

$$\begin{aligned} d\,(\mu_B,T) &= n\,(T)\,\mu_B + p\,(T)\,\mu_B^2 + r\,(T)\,\mu_B^3, \\ k\,(\mu_B,T) &= s\,(T)\,\mu_B + v\,(T)\,\mu_B^2 + w\,(T)\,\mu_B^3, \\ m\,(\mu_B,T) &= \alpha\,(T)\,\mu_B + \beta\,(T)\,\mu_B^2 + \eta\,(T)\,\mu_B^3\,. \end{aligned} \tag{6}$$

Lastly, the T dependence in the above coefficients fit via smooth functional dependencies resulting in

$$\begin{aligned} n\,(T) &= -0.04 + 2.3T - 12.8T^2, \\ p\,(T) &= 23.66 - 354T + 1175T^2, \\ r\,(T) &= -54.3 + 742.6T - 2350T^2, \\ s\,(T) &= -22.11 + 808.7T - 11604.4T^2 \\ &\quad +81700T^3 - 282480T^4 + 384116T^5, \\ v\,(T) &= -1.6 - 121.7T + 1775T^2 - 5516T^3, \\ w\,(T) &= -9.874 + 469T - 4371.5T^2 + 11000T^3, \\ \alpha\,(T) &= 84.784 - 3028.6T + 42434T^2 \\ &\quad -291390T^3 + 981000T^4 - 1295400T^5, \\ \beta\,(T) &= 59.64 - 726.46T + 1093.4T^2 + 4256T^3, \\ \eta\,(T) &= -73.9 + 458.66T + 2450T^2 - 12348T^3\,. \end{aligned} \tag{7}$$

A comparison between this parametrization and the explicitly calculated rates is shown in Fig. 1. We find that the parametrization reproduces the calculated rates with an accuracy better than 20%.

As a final test of the reliability of our fits, the "predictions" from the parametrization are compared to the calculated rates at μ_B = 0.3 GeV, a value not used in the fitting procedure. The deviation between parametrization and calculation is found to be very similar to fitted cases. Therefore, we conclude that our parameterized photon rates lie within the 20% error margin (significantly smaller for the most part) established in the fits, for photon energies q_0=0.2-5 GeV, temperatures T=100-180 MeV, and baryon chemical potentials μ_B=0-0.4 GeV.

Processes of type $\pi N \to \pi N\gamma$ and $NN \to NN\gamma$ are included in the ρ spectral functions used in the fits above, but meson-meson Bremsstrahlung is not. Since pions are the most abundant mesons at the relevant temperatures, and their small mass renders the kinematics favorable for radiating off photons, the dominant source in the mesonic

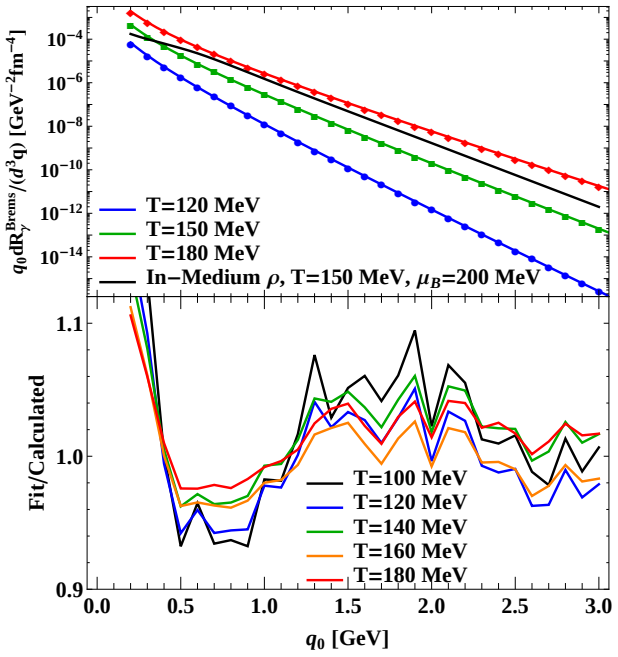

FIG. 2: Upper panel: Calculated thermal photon rates from $\pi\pi$ Bremsstrahlung (symbols) compared to their parametrization (colored lines). As a reference, we also display a rate from calculated in-medium ρ decays (black line). Lower panel: Ratio of the parameterized over calculated Bremsstrahlung rates.

sector is expected from $\pi\pi \to \pi\pi\gamma$ processes. The pertinent rates have been calculated in Ref. [28] in an effective hadronic model for S- and P-wave $\pi\pi$ (and πK) scattering. Special care was taken in maintaining EM gauge invariance in the presence of hadronic form factors, and in going beyond the often times applied soft-photon approximation. The analysis, however, focused on rather small photon energies, below 0.5 GeV, thus limiting the applicability of the provided parameterizations. Here, we carry these calculations to higher energies and generate suitable parameterizations.

Let us first compare the $\pi\pi$ Bremsstrahlung rate to the in-medium ρ decays discussed above. At typical hadronic temperatures of T=150 MeV the former exceeds the latter for q_0<0.4 GeV, but drops below it by about an order of magnitude for $q_0 \geq 1$ GeV, see Fig. 2. We note in passing that the contribution from πK Bremsstrahlung amounts to about 20% of the $\pi\pi$ one [28]. We have parameterized the latter using the ansatz

$$q_0 \frac{dR_\gamma^{\rm Brems}}{d^3q}(q_0;T) = \exp\left[\alpha_B(T) + \beta_B(T) q_0 + \gamma_B(T) q_0^2 + \delta_B(T)(q_0+0.2)^{-1}\right], \quad (8)$$

and found that with

$$\begin{aligned} \alpha_B(T) &= -16.28 + 62.45T - 93.4T^2 - 7.5T^3, \\ \beta_B(T) &= -35.54 + 414.8T - 2054T^2 + 3718.8T^3, \\ \gamma_B(T) &= 0.7364 - 10.72T + 56.32T^2 - 103.5T^3, \\ \delta_B(T) &= -2.51 + 58.152T - 318.24T^2 + 610.7T^3, \end{aligned} \quad (9)$$

the calculated rates are fitted within ∼5% for T=100-180 MeV and q_0=1-5 GeV, cf. lower panel of Fig. 2[1]. Noise is statistical in nature due to the calculated rates.

Chemical off-equilibrium (COE). The above parametrizations pertain to hadronic matter in chemical equilibrium (CE), i.e., for $\mu_B = -\mu_{\bar{B}}$ without any other chemical potentials (and therefore $\mu_B \equiv \mu_N$). However, in URHICs, hadro-chemical freezeout occurs well before kinetic freezeout, implying the emergence of effective chemical potentials, μ_i, to conserve the ratios of hadrons which are stable under strong decay, e.g., i=π, K, baryons and anti-baryons [32]. Since strong resonance formation reactions persist, one has μ_ρ=2μ_π, μ_Δ=$\mu_N + \mu_\pi$, etc. An extension of the rate parametrizations to fully incorporate the μ_i dependencies is not practical. However, their leading effect can be rather accurately captured by fugacity factors. For $\pi\pi$ Bremsstrahlung, this amounts to an extra overall factor of z_π^2 on the right-hand-side of Eq. (8), with z_π=exp(μ_π/T). The same factor also applies to Eq. (4) (representing the ρ fugacity), but additional amendments are needed, as we will discuss now.

Let us start from chemical freezeout, $T_{\rm ch}$, where $\mu_{\bar{B}}^{\rm ch} = -\mu_B^{\rm ch}$. For $T < T_{\rm ch}$, the separate conservation of baryon and anti-baryon number causes the effective anti-baryon chemical potential to rise with μ_B approximately as $\mu_{\bar{B}}(T) = \mu_{\bar{B}}^{\rm ch} + (\mu_B(T) - \mu_B^{\rm ch}) = \mu_B(T) - 2\mu_B^{\rm ch}$ [32]. This increase in $\mu_{\bar{B}}(T)$ over the CE case must be accounted for in the baryonic contributions to the rate. Toward this end, we define the ratio r by which the COE density of baryons plus anti-baryons is enhanced over the CE value,

$$r \equiv \frac{n_{B+\bar{B}}^{\rm COE}}{n_{B+\bar{B}}^{\rm CE}} = \frac{n_B(\mu_B) + n_{\bar{B}}(\mu_B - 2\mu_B^{\rm ch})}{n_B(\mu_B) + n_{\bar{B}}(-\mu_B)} = \frac{1 + {\rm e}^{-2\mu_B^{\rm ch}/T}}{1 + {\rm e}^{-2\mu_B/T}} . \quad (10)$$

Here, we have utilized the Boltzmann approximation, $n_B(\mu_B) \simeq n_B(0)\,{\rm e}^{\mu_B/T}$. The effective baryon chemical potential, $\mu_B^{\rm eff}$, to be used in the above photon rate, is then given by

$${\rm e}^{\mu_B^{\rm eff}/T} \equiv r\ {\rm e}^{\mu_B/T} \quad \Rightarrow \quad \mu_B^{\rm eff} = \mu_B + T\log(r) . \quad (11)$$

The thermal meson-induced photon emission in the ρ spectral function is mostly due to resonance formation,

[1] We note that when combining the present $\pi\pi$ Bremsstrahlung rates with the ones given in the appendix of Ref. [23], the $\rho \to \pi\pi\gamma$ and $\pi\pi \to \rho\gamma$ contributions in there need to be dropped to avoid double-counting.

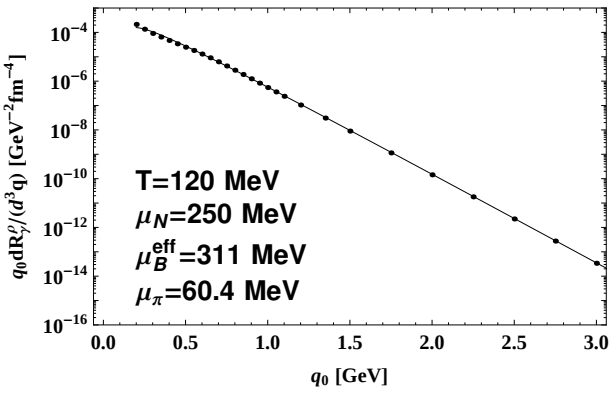

FIG. 3: Photon emission rates calculated from in-medium ρ's (points) compared to the parametrization of Eq. (4) evaluated with $\mu_B^{\rm eff}$ from Eq. (11) and an overall fugacity of z_π^3.

$P\rho \to M \to P\gamma$ [27]. With P=π being the dominant contribution, one picks up another factor of z_π (in addition to the z_π^2 of the ρ). The meson gas sources only prevail at higher q_0, while the baryon-induced ones take over toward smaller q_0. However, many of the baryons are in excited states which carry larger chemical potentials than the nucleon, e.g., μ_Δ=$\mu_N + \mu_\pi$, $\mu_{N(1520)}$=$\mu_N + 1.45\mu_\pi$, etc. It turns out that an extra overall factor of z_π approximately accounts for the chemically enhanced resonance abundances.

To summarize the overall effect of the COE extension, the function F^ρ in Eq. (4) should be replaced as

$$F^\rho \to z_\pi^3 \; F^\rho\left(q_0; \mu_B^{\rm eff}, T\right), \qquad (12)$$

while the $\pi\pi$ Bremsstrahlung rate receives an overall factor of z_π^2. These amendments yield rather accurate agreements, typically within less than 10% (see, e.g., Fig. 3), largely determined by the intrinsic uncertainty of the equilibrium parametrizations.

Conclusion. We have constructed universal parametrizations for microscopic photon emission rates from in-medium ρ mesons and $\pi\pi$ Bremsstrahlung over a range of photon energies, temperatures, and baryon-chemical potentials relevant to applications in URHICs. Our parametrizations reproduce the calculated rates within 20% (mostly within 10%). We have confirmed that $\pi\pi$ Bremsstrahlung is appreciable for energies $q_0 < 1\,$GeV, but subleading above. We have devised a prescription to extend the equilibrium parameterizations to capture the effects of chemical off-equilibrium as encountered in URHICs. We believe that these parametrizations will be useful in calculations of thermal photon emission within different medium evolution models, and thus contribute to a better understanding of pertinent observables.

This work has been supported by the U.S. NSF under REU-grant No. PHY-1263281 and grant No. PHY-1306359, and by the Humboldt Foundation (Germany).

* Electronic address: mrheffernan@email.wm.edu
† Electronic address: pmhohler@comp.tamu.edu
‡ Electronic address: rapp@comp.tamu.edu

[1] R. Rapp, J. Wambach and H. van Hees, in *Relativistic Heavy-Ion Physics*, edited by R. Stock and Landolt Börnstein (Springer, Berlin, 2010), New Series **I/23A**, p. 4-1; [arXiv:0901.3289 [hep-ph]].
[2] C. Gale, in *Relativistic Heavy-Ion Physics*, edited by R. Stock and Landolt Börnstein (Springer, Berlin, 2010), New Series **I/23A**, p. 6-3; [arXiv:0904.2184 [hep-ph]].
[3] A. Adare *et al.* [PHENIX Collaboration], Phys. Rev. Lett. **104**, 132301 (2010).
[4] A. Adare *et al.* [PHENIX Collaboration], Phys. Rev. Lett. **109**, 122302 (2012).
[5] M. Wilde *et al.* [ALICE Collaboration], Nucl. Phys. A **904-905**, 573c (2013).
[6] D. Lohner *et al.* [ALICE Collaboration], J. Phys. Conf. Ser. **446**, 012028 (2013).
[7] C. Yang *et al.* [STAR Collaboration], Nucl. Phys. A (2014); [arXiv:1408.2371 [hep-ex]].
[8] F. M. Liu, T. Hirano, K. Werner and Y. Zhu, Phys. Rev. C **80**, 034905 (2009).
[9] H. van Hees, C. Gale and R. Rapp, Phys. Rev. C **84**, 054906 (2011).
[10] H. Holopainen, S. Räsänen and K. J. Eskola, Phys. Rev. C **84**, 064903 (2011).
[11] M. Dion *et al.*, Phys. Rev. C **84**, 064901 (2011).
[12] P. Mohanty *et al.*, Phys. Rev. C **85**, 031903 (2012).
[13] C. Shen, U. W. Heinz, J. F. Paquet and C. Gale, Phys. Rev. C **89**, 044910 (2014).
[14] O. Linnyk, W. Cassing and E. L. Bratkovskaya, Phys. Rev. C **89**, 034908 (2014).
[15] A. Bzdak and V. Skokov, Phys. Rev. Lett. **110**, 192301 (2013).
[16] A. Monnai, Phys. Rev. C **90**, 021901 (2014).
[17] C. Gale *et al.*, arXiv:1409.4778 [hep-ph].
[18] L. McLerran, arXiv:1411.1548 [hep-ph].
[19] J.I. Kapusta, P. Lichard and D. Seibert, Phys. Rev. D **44**, 2774 (1991); [Erratum-ibid. D **47**, 4171 (1993)].
[20] L. Xiong, E. V. Shuryak and G. E. Brown, Phys. Rev. D **46**, 3798 (1992).
[21] J. V. Steele, H. Yamagishi and I. Zahed, Phys. Lett. B **384**, 255 (1996).
[22] S. Sarkar *et al.*, Nucl. Phys. A **634**, 206 (1998).
[23] S. Turbide, R. Rapp and C. Gale, Phys. Rev. C **69**, 014903 (2004).
[24] R. Rapp, G. Chanfray and J. Wambach, Nucl. Phys. A **617**, 472 (1997).
[25] M. Urban, M. Buballa, R. Rapp, and J. Wambach, Nucl. Phys. A **673**, 357 (2000).
[26] R. Rapp and J. Wambach, Eur. Phys. J. A **6** 415, (1999).
[27] R. Rapp and C. Gale, Phys. Rev. C **60**, 024903 (1999).
[28] W. Liu and R. Rapp, Nucl. Phys. A **796**, 101 (2007).
[29] L.D. McLerran and T. Toimela, Phys. Rev. D **31**, 545 (1985).
[30] R. Rapp, Adv. High Energy Phys. **2013**, 148253 (2013).
[31] R. Rapp, H. van Hees and M. He, Nucl. Phys. A (2014); [arXiv:1408.0612 [nucl-th]].
[32] R. Rapp, Phys. Rev. C **66**, 017901 (2002).